

Research Article

Actin patch assembly proteins Las17p and Sla1p restrict cell wall growth to daughter cells and interact with *cis*-Golgi protein Kre6p

Huijuan Li, Nicolas Pagé and Howard Bussey*

Department of Biology, McGill University, Montreal, Canada H3A 1B1

*Correspondence to:

Howard Bussey, Department of Biology, McGill University, Montreal, Quebec, Canada H3A 1B1.

E-mail: hbusse@po-box.mcgill.ca

Abstract

The cytoplasmic tail of Kre6p, a Golgi membrane protein involved in cell wall synthesis, interacts with the actin patch assembly components Las17p and Sla1p in a two-hybrid assay, and Kre6p co-immunoprecipitates with Las17p. Kre6p showed extensive co-localization with Och1p-containing *cis*-Golgi vesicles. The correct localization of Kre6p requires its cytoplasmic tail, Las17p, Sla1p and Vrp1p, suggesting that the cytoplasmic tail of Kre6p acts as a receptor, linking this *cis*-Golgi protein to Las17p and Sla1p. The actin patch assembly mutants *las17* Δ , *sla1* Δ and *vrp1* Δ showed elevated levels of cell wall β -1,6-glucan, and mutant cells were capable of only a limited number of cell divisions compared to wild-type. EM image analysis and β -1,6-glucan localization indicated abnormal wall proliferation in the mother cells of these mutants. The pattern of cell wall hypertrophy indicates a failure to restrict cell wall growth to the bud. Copyright © 2002 John Wiley & Sons, Ltd.

Received: 21 February 2002

Accepted: 14 June 2002

Keywords: Golgi vesicle receptor; cortical actin patch assembly; cell wall synthesis; β -1,6-glucan localization; mother–daughter asymmetry

Introduction

The coupling of cell wall synthesis with polarized growth is a critical process for fungal cells, providing spatial and temporal regulation of cellular expansion. In yeast, the actin cytoskeleton plays a central role in polarized and isotropic cell growth, providing a scaffold for many processes, including cell wall synthesis, localized membrane growth and endocytosis. The actin-directed polarized growth of a daughter cell leads to a mother–daughter growth asymmetry, resulting in the formation of a new cell.

Filamentous actin is organized primarily into cortical patches and actin cables in yeast (reviewed by Pruyne and Bretscher, 2000). In cortical patch assembly mutants, such as *myo3* Δ *myo5* Δ , *act1-1*, *sla2* Δ /*end4* Δ , *pan1-4*, *end3* Δ , *sla1* Δ and *vrp1* Δ /*end5* Δ , mother cells can generate multi-layered cell walls (Goodson *et al.*, 1996; Mulholland *et al.*, 1997; Ayscough *et al.*, 1999; Tang *et al.*, 2000;

Naqvi *et al.*, 2001). Similar multi-layered cell walls were also reported in double and triple mutants of *INP51*, *INP52*, *INP53*, an essential family of inositol polyphosphate 5-phosphatases involved in vesicle trafficking, membrane structure and cell wall formation (Srinivasan *et al.*, 1997; Stolz *et al.*, 1998). Excessive cell wall deposition also occurs in mother cells when some proteins are overexpressed, e.g. the Sla1p C-terminal repeats (Tang *et al.*, 2000) and the stress sensor Mid2p in *pfy1* Δ cells (Marcoux *et al.*, 1998). The basis for this mother cell wall hypertrophy is not well understood but, as it is allele-specific for some actin mutants, the process probably depends upon proteins specifically interacting with the actin cytoskeleton (Tang *et al.*, 2000). Actin-mediated processes, such as endocytosis, the regulation of polarized and isotropic growth and the mother–daughter asymmetry establishment, are potentially involved. Such defects in mother–daughter cell wall asymmetry resulting

in cell wall hypertrophy offer a way to study the integration of wall synthesis with polarized growth.

The *Saccharomyces cerevisiae* cell wall is an essential organelle composed of mannoproteins, β -1,3-glucan, β -1,6-glucan and chitin. β -1,6-glucan is cross-linked to β -1,3-glucan, chitin and wall mannoproteins, with a key role in maintaining wall integrity (Kollár *et al.*, 1997). Kre6p is a Golgi membrane protein required for normal β -1,6-glucan levels in the cell wall (Roemer and Bussey, 1991; Roemer *et al.*, 1994). *SKN1* encodes a related protein topologically similar to Kre6p (Roemer *et al.*, 1993). Hydrophobic cluster analysis showed that the luminal domains of Kre6p and Skn1p have significant similarities to family 16 glycoside hydrolases, suggesting that they are glucosyl hydrolases or transglucosylases (Montijn *et al.*, 1999). *SKN1* acts as a multicopy suppressor of a *kre6* null, and a *skn1* null shows strong synthetic defects with *kre6* Δ , being lethal in some backgrounds. *KRE6* and *SKN1* gene expression is differentially regulated during the cell cycle (Igual *et al.*, 1996; Spellman *et al.*, 1998).

In this study, we find genetic and physical interactions between the *cis*-Golgi membrane protein Kre6p, and the actin patch components Las17p/Bee1p (Li, 1997) and Sla1p (Ayscough *et al.*, 1999). Our data also indicate that actin patch

assembly components play critical roles in restricting cell wall growth to daughter cells.

Materials and methods

Yeast and bacterial strains and culture conditions

The *S. cerevisiae* strains used in this study are summarized in Table 1 and the plasmid constructs used in this study are summarized in Table 2. Oligonucleotide primers are listed in Table 3. Standard growth conditions and media (YEPD, YNB) for yeast cells were used (Bussey *et al.*, 1982). Genetic crosses, sporulation of diploids and dissection of tetrads were performed using standard methods (Sherman *et al.*, 1982). Yeast transformations were carried out in two ways: transformation of plasmids was performed using the one-step method of Chen *et al.* (1992), whereas transformation of PCR products, restriction digest-derived fragments for the purpose of genetic disruptions or of the genomic library for the two-hybrid screen, was performed using the method of Gietz *et al.* (1995). Transformants were selected on synthetic minimal medium with auxotrophic supplements, with the exception of selection using the *kanMX2* module, which used YEPD containing 200 μ g/ml geneticin (Gibco). Plasmids were propagated using

Table 1. Yeast strains used in this study

Strain	Genotype	Source
SEY6210 diploid	<i>leu2-3 112 ura3-52 his3-Δ200 lys2-801 trp1-Δ901 suc2-Δ9 Mata/a</i>	S.D. Emr
TR92	<i>kre6::HIS3 leu2-3 112 ura3-52 his3-Δ200 lys2-801 trp1-Δ901 suc2-Δ9 Mata</i>	Roemer <i>et al.</i> , 1991
HAB925	<i>skn1::kanMX2 leu2-3 112 ura3-52 his3-Δ200 lys2-801 trp1-Δ901 suc2-Δ9 Mata</i>	This study
HAB926	<i>kre6::HIS3 skn1::kanMX2 leu2-3 112 ura3-52 his3-Δ200 lys2-801 trp1-Δ901 suc2-Δ9 Mata/a</i>	This study
BY4741	<i>his3Δ1 leu2Δ0 met15Δ0 ura3Δ0 Mata</i>	Yeast genome deletion project*
BY4742	<i>his3Δ1 leu2Δ0 lys2Δ0 ura3Δ0 Mata</i>	
BY4743	<i>BY4741/4742 Mata/a</i>	
MC75	<i>thr5 met Mata</i>	M.W. Clark
MC76	<i>lys1 cry1 Mata</i>	M.W. Clark
Y1003	A diploid W303(<i>ura3-1 leu2-3 his3-11 trp1-1 ade2-1 can1 100 Mata/a</i>) derivative carrying <i>URA3::lexAop-laz/URA3::lexAop-ADE2 reporter</i>	Anderson <i>et al.</i> , 1998
Y2312	A W3031A strain expressing <i>Las17p-HA/Bee1p-HA (BEE1::3HA-TRP)</i> , <i>ura3-1 leu2-3-112 trp1-1 ade2-1 can1-100</i>	Evangelista <i>et al.</i> , 2000

* All genes were disrupted with the *kanMX4* module and strains have the following genotype: *his3 Δ 1 leu2 Δ 0 met15 Δ 0 ura3 Δ 0* for BY4741 *Mata*, or *his3 Δ 1 leu2 Δ 0 lys2 Δ 0 ura3 Δ 0* for BY4742 *Mata*, except for *las17::kanMX4*, which was obtained from deletion diploid strain BY4743 by sporulation and tetrad dissection at room temperature and is of genotype *his3 Δ 1 leu2 Δ 0 met15 Δ 0 lys2 Δ 0 ura3 Δ 0*. The null deletion strains of *arc18*, *arp6*, *bnl1*, *dec1*, *end3*, *kre6*, *myo3*, *myo4*, *rvs161*, *rvs167*, *sac6*, *sla1*, *sla2*, *she4*, *vrp1* and *twf1* were also used.

Table 2. Plasmid constructs used in this study*

Plasmid	Description	Reference
pRS315	<i>CEN6 LEU2</i>	Sikorski <i>et al.</i> , 1989
pRS316	<i>CEN6 URA3</i>	Sikorski <i>et al.</i> , 1989
pRS425	2μ <i>LEU2</i>	Christianson <i>et al.</i> , 1992
pRS426	2μ <i>URA3</i>	Christianson <i>et al.</i> , 1992
pEG202-NLS	2μ <i>HIS3</i>	C. Boone, University of Toronto
pBD KRE6 (1–137 aa)	Kre6p 1–137 aa <i>EcoRI</i> fragment in pEG202-NLS	
pBD SKN1 (1–166 aa)	Skn1p 1–166 aa <i>BamHI/EcoRI</i> fragment in pEG202-NLS	
pRS316 KRE6	Kre6p; <i>BamHI/Sall</i> fragment in pRS316	Roemer <i>et al.</i> , 1991
pRS316 KRE6 Δ 1	Kre6p Δ 1; <i>BamHI/Sall</i> fragment in pRS316 with deletion of 1–137 aa at the N-terminus of Kre6p	
pRS316 KRE6 Δ 2	Kre6p Δ 2; <i>BamHI/Sall</i> fragment in pRS316 with deletion of 1–248 aa at the N-terminus of Kre6p	
pRS316 KRE6 Δ 1–ST1	Skn1p N-terminal <i>NotI</i> fragment (1–166 aa) was subcloned at the N-terminus of pRS316 KRE6 Δ 1	
pRS316 KRE6 Δ 2–ST2	Skn1p N-terminal <i>NotI</i> fragment (1–288 aa) was subcloned at the N-terminus of pRS316 KRE6 Δ 2	
pRS426 KRE6	Kre6p; <i>BamHI/Sall</i> fragment in pRS426	
pRS426 KRE6 Δ 1	Kre6p Δ 1; <i>BamHI/Sall</i> fragment of pRS316 KRE6 Δ 1 in pRS426	
pRS426 KRE6 Δ 2	Kre6p Δ 2; <i>BamHI/Sall</i> fragment of pRS316 KRE6 Δ 2 in pRS426	
pRS426 KRE6–GFP	GFP <i>NotI</i> fragment was subcloned at the N-terminus of pRS426 KRE6	
pRS426 KRE6 Δ 1–GFP	GFP <i>NotI</i> fragment was subcloned at the N-terminus of pRS426 KRE6 Δ 1	
pRS426 KRE6 Δ 2–GFP	GFP <i>NotI</i> fragment was subcloned at the N-terminus of pRS426 KRE6 Δ 2	
pRS425 KRE6–GFP	Kre6pGFP; <i>BamHI/Sall</i> fragment in pRS425	
pRS426 MID2–GFP	GFP was fused at the C-terminus of Mid2p in pRS426	Ketela <i>et al.</i> , 1999
pRS315 GFP–FKS1		Dijkgraaf <i>et al.</i> , 2002
pRS316 CHS5–GFP	Personal communication	C. Boone, University of Toronto
pOH	Och1p–HA	Harris and Waters, 1996
pRS316 KEX1–HA		Lussier <i>et al.</i> , 1995
pRHL–HA ₃	VRG4–HA ₃ / <i>URA3/CEN6</i>	Poster and Dean, 1996

* All resulting plasmid constructs from this study were confirmed by DNA sequencing.

the *E. coli* strain DH10B, except for the preparation of uracil-containing DNA for mutagenesis, which was done using the *E. coli* strain CJ236 (dut⁻ ung⁻F'). Bacterial cells were cultured and transformed using standard media and methods (Sambrook *et al.*, 1989).

DNA purification and recombinant DNA techniques

Yeast DNA was isolated by the method of Hoffman and Winston (1987). Plasmid minipreps were prepared from *E. coli* via the boiling method or by the alkaline lysis method described by Sambrook *et al.* (1989). Restriction endonucleases, calf intestinal alkaline phosphatase, T4 DNA ligase, sequenase, T4 polynucleotide kinase, and the Gene 32 protein were from Bethesda Research Laboratories Inc.

(Gaithersburg, MD), Pharmacia LKB Biotechnology (Piscataway, NJ), New England Biolabs (Beverly, MA), Boehringer Mannheim Biochemicals (Indianapolis, IN) or US Biochemicals (Cleveland, OH), and were used according to the manufacturers' instructions.

Plasmid constructions

Site-directed mutagenesis introducing *NotI* or *NotI*-ATG was performed via the method of Kunkel *et al.* (1987), using the primers KRE6-*NotI*-1bp, KRE6-*NotI* ATG-412bp and KRE6-*NotI* ATG-745bp (listed in Table 3). Single-stranded, uracil-containing DNA of pRS316 KRE6 (Table 2) prepared according to Sambrook *et al.* (1989), was used as the template.

Table 3. Oligonucleotide sequences used in this study

Name	Sequence 5'–3'*
SKN1–kanMX2- 5'	CAT TCC AAC AGC GAA AAT AGT GTT TCC GGA AGC GAA AAC TCC <u>GAT ATC AAG CTT GCC TCG</u>
SKN1–kanMX2- 3'	TGG GAA AGT ATA TCC AGC CTG TTC CCA ATC AGT TAA ATT GGC <u>GTC GAC ACT GGA TGG CGG</u>
SKN1–test 5'	ATA TCG CTC TGC GAA CCG
kanMX2 internal	CAACAGGCCAGCCATTAC
5'-BamHI–KRE6 (1–5 aa)	CGC GGA TCC GCA TGC CTT TGA GAA AT
3'-BamHI–KRE6 (244–248 aa)	CGC GGA TCC GCC CTT TTA TCC ATG TA
5'-EcoRI–SKN1 (1–5 aa)	CCG GAA TTC CGG ATG TCT GTG CGA AAC
3'-SKN1–BamHI (162–166 aa)	CGC GGA TCC GCT GAA GAA GGA TGA GA
5'-KRE6–EcoRI (138–143 aa)	CCG GAA TTC AAT TCT AAT TTA TCG AAG
KRE6–NotI 1 bp	CAC TCC TTT ACT CTA GCG GCC GCA ATG CCT TTG AGA AAT
KRE6–NotI ATG 412 bp	TCT TCT CCT TCT TTG GCG GCC GCA ATG AAT TCT AAT TTA TCG
KRE6–NotI ATG 745 bp	TAC ATG GAT AAA AGG GCG GCC GCA ATG TCT GCT AGT GGG CTA
5'-SKN1–NotI 1 bp	AAA CAA TAG CAG AAT GCG GCC GCA ATG TCT GTG CGA AAC
5'-SKN1–NotI ATG 498 bp	TCT CAT CCT TCT TCA GCG GCC GCA ATG AAT AAT ATG AGT AGC
5'-SKN1–NotI ATG 865 bp	CAC ATG GAT AGA AGA GCG GCC GCA ATG TCT TTC TTG GGG CTT
3'-SKN1–NotI 498 bp	GCT ACT CAT ATT ATT TGC GGC CGC TGA AGA AGG ATG AGA
3'-SKN1–NotI 864 bp	GAA AGA TGC GGC CGC TCT TCT ATC CAT GTG
5'-GFP–NotI	GTA GAA AAA GCG GCC GCA ATG AGT AAA GGA GAA
3'-GFP–NotI	ATT CTA CGA ATG CTA TGC GGC CGC TTT GTA TAG TTC ATC

* Underlined sequences indicate the *KanMX2* module and bold sequences indicate restriction sites.

Gene disruption

Mutants were either obtained from the Yeast Genome Deletion Project (see Table 1) or by gene disruptions performed on a SEY6210-derived diploid, followed by sporulation, tetrad dissection and mating type analysis using the tester strains MC75 and MC76 (Table 1) to obtain disrupted haploid progeny of known mating type. The *skn1::kanMX2* was prepared by PCR-based disruption with the *kanMX2* module, as described by Wach *et al.* (1994), using the PCR oligonucleotide primers SKN1-kanMX2-5' and SKN1-kanMX2-3' (shown in Table 3) and the pFA6 *kanMX2* plasmid as a template. Integrants in HAB925 were verified by PCR analysis using test primers corresponding to the 5' upstream genomic sequence of *SKN1*, SKN1-test-5', and the internal reverse primer derived from the *kanMX2* module, kanMX2 internal (Table 3). The *kre6Δskn1Δ* diploid strain HAB926 was prepared by crossing appropriate haploid strains. Viability tests of *kre6Δlas17Δ*, *kre6Δsla1Δ* and *kre6Δvrp1Δ* were performed on progeny of crosses of the appropriate haploid strains obtained following sporulation and tetrad dissection.

Immunofluorescence microscopy

Co-visualization of Kre6p-GFP and other Golgi proteins

Cells from exponentially growing cultures were used. Wild-type cells containing pRS425 KRE6-GFP and pRHL-HA (VRG4-HA, Poster and Dean, 1996), pRS425 KRE6-GFP and pOH (OCH1-HA, Harris and Waters, 1996), or pRS425 KRE6-GFP and pRS316 KEX1-HA (Lussier *et al.*, 1995) (Table 2) were fixed with 3.7% formaldehyde in TBST (10 mM Tris, pH 8.0, 150 mM NaCl, 0.05% Tween) for 30 min, washed twice with TBST and digested with zymolyase 100T (Seikagaku, Japan) for 25 min at room temperature. Double immunofluorescence was performed using 1:50 monoclonal HA.11 (Berkeley Antibody Company) and a specific rabbit anti-GFP (green fluorescence protein) antibody (Molecular Probes) in TBST containing 1% BSA. Texas red-conjugated goat anti-mouse IgG and Oregon green-conjugated goat anti-rabbit IgG (Molecular Probes) were used as the secondary antibodies in TBST containing 1% BSA. Cells were visualized using a Zeiss fluorescence microscope (Zeiss, Germany) equipped with a Spot Digital Camera (Diagnostic Instruments, Michigan, USA).

Localization of β -1,6-glucan

To view new β -1,6-glucan deposition in cells, we modified the method of Tkacz and Lampen (1972). Logarithmic cultures (1 ml), grown in YEPD at room temperature, were collected and washed twice with TBST. Cells were then incubated in TBST containing 1% BSA for 30 min. The existing β -1,6-glucan was blocked by incubating cells in a 1:100 dilution of a specific rabbit anti- β -1,6-glucan antibody for 1 h (Lussier *et al.*, 1998) and a 1:20 dilution of horseradish peroxidase-conjugated anti-rabbit secondary antibody (Amersham) for 1 h in TBST containing 1% BSA. Cells were then grown for another 2–3 h at room temperature, and immunofluorescence was performed as above using 1:100 anti- β -1,6-glucan antibody and 1:20 Oregon green-conjugated goat anti-rabbit IgG as the secondary antibody. Cells were visualized using a Zeiss fluorescence microscope equipped with a Spot digital camera. Control experiments were performed by directly incubating the cells with Oregon green-conjugated goat anti-rabbit IgG after horseradish peroxidase-conjugated anti-rabbit secondary antibody treatment without further growth, and under these conditions cells did not fluoresce.

Two-hybrid analysis

Two-hybrid studies were performed according to Chien *et al.* (1991), using the diploid W303 derivative, Y1003, as a host (Table 1; Anderson *et al.*, 1998). Strain Y1003 was sequentially transformed with the DNA-binding domain fusion pBD KRE6 (1–137 aa), constructed in pEG202 (Gyuris *et al.*, 1993) with a nuclear localization signal (NLS, pEG202-NLS, Boone, C., personal communication; Table 2) and the FRYL library (Fromont-Racine *et al.*, 1997). Positives selected on his⁻ leu⁻ ade⁻ were assayed for β -galactosidase activity according to Gietz *et al.* (1997).

Immunoprecipitation

Total cell lysates were made from exponentially growing cultures expressing Kre6p–GFP and Las17p–HA, or untagged controls, by vortexing with glass beads in 10 mM Tris–HCl and 1 mM EDTA containing protease inhibitors (Boehringer Mannheim, Germany). Kre6p–GFP was gently solubilized according to Jungmann and Munro (1998)

at room temperature for 1 h. Immunoprecipitation was performed as described by Jungmann and Munro (1998), using HA.11 antibody (1:150 dilution) in a volume of 1.2 ml containing 2–5 mg cellular protein. Precipitates and supernatants were then subjected to Western blot analysis.

Western blot analysis

Protein samples were analysed by sodium dodecyl sulphate–polyacrylamide gel electrophoresis (SDS–PAGE; Laemmli, 1970) using 8% polyacrylamide gels, and then transferred to Hybond-C nitrocellulose membranes (Amersham, Oakville, ON, Canada). Immunoblotting of GFP-fused Kre6p, Kre6p Δ 1 and Kre6p Δ 2 was performed using a 1:2000 dilution of a specific rabbit anti-GFP antibody and a 1:2000 dilution of horseradish peroxidase-conjugated anti-rabbit secondary antibody, and was subsequently detected using an enhanced chemiluminescence procedure (Amersham). Immunoblotting of Las17p–HA was performed using a 1:2000 dilution of HA.11 monoclonal antibody and a 1:2000 dilution of horseradish peroxidase-conjugated anti-mouse secondary antibody.

Localization of Kre6p–GFP derivatives

Cells were from exponentially growing liquid cultures or from an agar plate incubated at 30°C or room temperature overnight. Cells containing various GFP-fusion constructs (Table 2) were spotted onto a microscope slide, covered with a coverslip and visualized using a Zeiss fluorescence microscope equipped with a Spot digital camera.

Cell wall analysis

Resistance of yeast strains to K1 killer toxin was determined as described previously (Brown *et al.*, 1993). The levels of alkali-insoluble cell wall β -1,3- and β -1,6-glucan were determined as described by Shahinian *et al.* (1998), except that values were calculated as μ g glucan/mg total cellular protein and reported as percentages (WT = 100%) to facilitate comparison. Protein was measured by the dye-binding assay of Bradford (1976; BioRad, Mississauga, ON, Canada).

Cell lineage analysis

In each case, nine newly budded daughter cells were separated from their mother cells on YEPD plates, and these virgin daughters were grown at room temperature on YEPD plates for 60 h over 6 days (kept at 4°C overnight). Cell divisions were monitored on a dissector (Singer Instruments, UK) every 1.5 h for the first 4 days, and every 2 h for the last 2 days, with daughter cells successively removed from the mother cells by micromanipulation until the mother cells failed to bud.

Electron microscopy and image analysis

Yeast cells were grown in liquid culture at room temperature to stationary phase and fixed in an equal volume of 2.5% glutaraldehyde in 0.1 M sodium cacodylate buffer (0.1 M cacodylate in 0.1% CaCl₂, pH 7.4) at room temperature for 1 h. After three washes with 0.1 M sodium cacodylate buffer, cells were fixed in 1% OsO₄ for 1.5 h, followed by several water washes, dehydration in an acetone:water series, then embedded in Epon 812 resin. Ultrathin sections were stained with uranyl acetate and lead citrate and viewed in a JEOL 2000 electron microscope. EM images were analysed from random fields of wild-type and mutant cells. Different types of cells were grouped, and counted according to the number of cell wall layers in the mother cells.

Results

Localization of Kre6p to *cis*-Golgi vesicles

Kre6p is a type II Golgi membrane protein, with a phosphorylated cytoplasmic N-terminal domain (Figure 1A) and a luminal glucosyl hydrolase-like C-terminal domain (Roemer and Bussey, 1991; Roemer *et al.*, 1994; Montijn *et al.*, 1999). An N-terminal fusion of GFP with wild-type Kre6p was made to more precisely assess the Golgi location of Kre6p (Table 2, Figure 1B). Attempts to visualize Kre6p-GFP expressed from a centromeric plasmid were unsuccessful, so a high copy plasmid was used. Co-visualization of Kre6p-GFP and Vrg4p-HA, a UDP-mannose transporter widely distributed throughout Golgi compartments (Poster and Dean, 1996), revealed 75% co-localization of

Kre6p with Vrg4p in a total of 15 cells examined, although over 50% of Vrg4p vesicles contained no Kre6p (139 spots counted for Kre6p-GFP and 228 counted for Vrg4p-HA, in which 104 spots co-localized) (data not shown). Och1p and Kex1p, *cis*- and late-Golgi proteins, respectively, were also used as markers. Co-visualization showed that 88% of Kre6p spots co-localized with Och1p (19 cells examined, 90 spots counted for Kre6p-GFP and 109 counted for Och1p-HA, in which 79 spots co-localized) (Figure 2A), whereas only 23% of Kre6p spots co-localized with Kex1p (23 cells examined, 258 spots counted for Kre6p-GFP and 249 counted for Kex1p-HA, in which 60 spots co-localized) (Figure 2B). We therefore concluded that Kre6p is localized to *cis*-Golgi vesicles.

Las17p and Sla1p interact with the cytoplasmic tail of Kre6p in a two-hybrid assay

To determine a possible role for the long 248 amino acid residue cytoplasmic tail of Kre6p, we performed a deletional analysis of *KRE6*. The cytoplasmic tail is required for Kre6p function, since Kre6p Δ 1, a partial deletion of the tail (residues 1–137), can only partially complement the *kre6* null K1 toxin resistance phenotype, and Kre6p Δ 2, a complete deletion of the tail (residues 1–248), fails to complement this phenotype (Figure 1B). However, both Kre6p Δ 1 and Kre6p Δ 2 retained some function, as they rescued the lethality of the *kre6* Δ *skn1* Δ double mutant and partially restored β -1,6-glucan levels in a *kre6* Δ mutant (Figure 1B). A fusion replacing the Kre6p cytoplasmic domain with that of Skn1p did not complement the toxin resistance phenotype of a *kre6* null, suggesting distinct functions for these domains (Figure 1B bottom).

To identify possible interacting proteins, the N-terminal 137 amino acid residue cytoplasmic tail region of Kre6p was fused to a GAL4 DNA-binding domain and used as a bait in a two-hybrid screen, which identified Las17p and Sla1p (Table 4). Two clones of *LAS17* contained the identical fragment spanning amino acid residues 168–400 of the protein (Table 4). Three clones of *SLA1* were identified (Table 4). The smallest fragment contained amino acid residues 475–576 of the protein (Table 4), a region not known to interact with other proteins, and which contains part of a domain termed SHD1, conserved with the *Sz. pombe* homologue (Ayscough

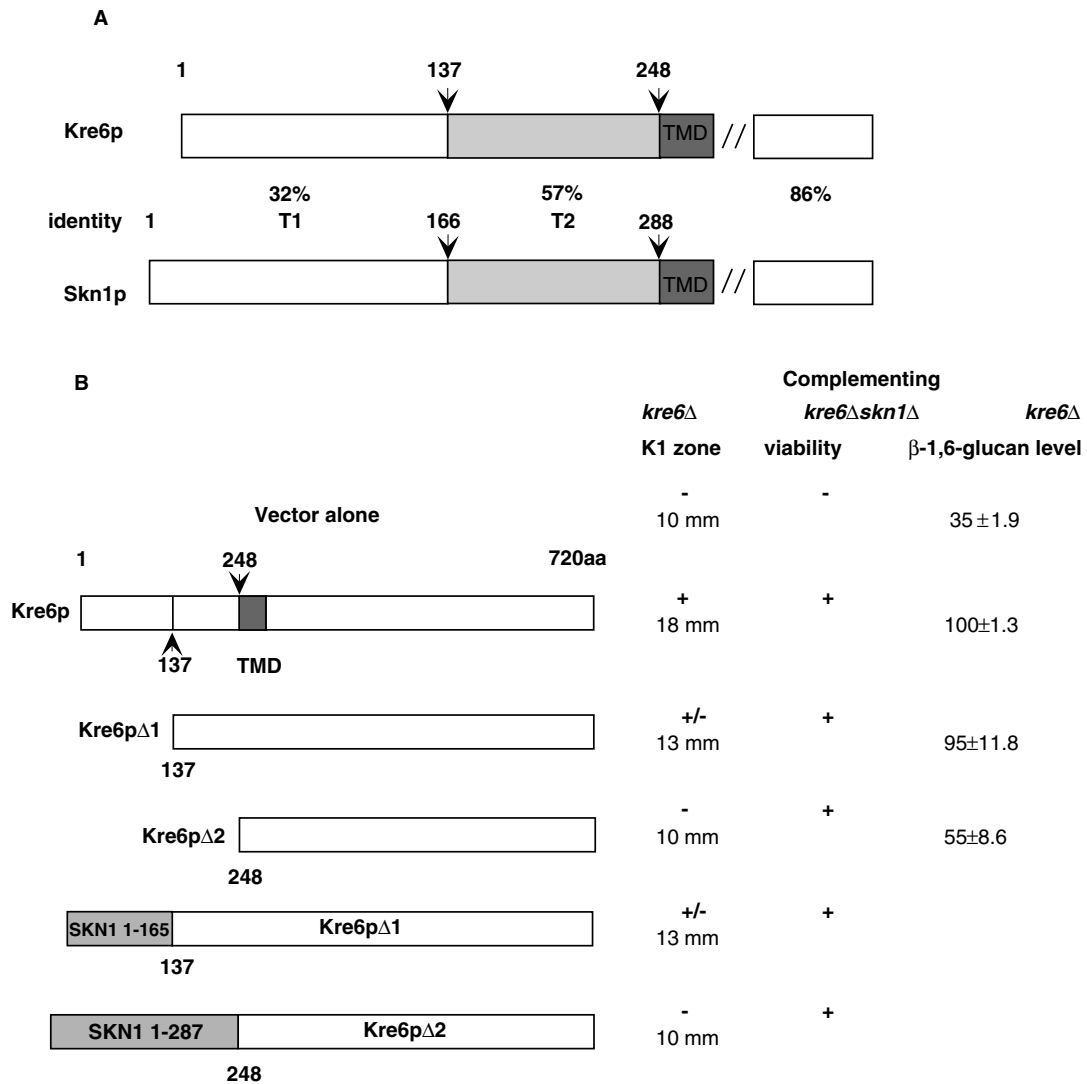


Figure 1. (A) Diagram of the cytoplasmic tails of Kre6p and Skn1p, showing two regions, T1 and T2, differing in amino acid sequence identity. (B) Kre6p cytoplasmic tail analysis. Function of the tail was determined by measuring the KI toxin killing zone diameter and by the ability to restore viability to the synthetically lethal *kre6Δskn1Δ* mutant and to complement the β -1,6-glucan defect in a *kre6Δ* mutant. GFP was fused in each case at the N-terminus of the Kre6p, Kre6pΔ1 and Kre6pΔ2 constructs shown in (B). These GFP constructs gave KI toxin complementation results similar to their Kre6p counterparts (data not shown). Alkali-insoluble β -1,6-glucan levels expressing these GFP constructs in *kre6Δ* mutants are shown as percentages. Values represent mean \pm SD

et al., 1999). The Skn1p cytoplasmic tail did not interact with these Las17p or Sla1p fragments (see Table 4, footnote), providing a negative control for specificity of the Kre6p interaction. Double mutants of *kre6Δsla1Δ* or *kre6Δlas17Δ* were synthetically lethal (data not shown). To further test the Kre6p and Las17p interaction, we found that Kre6p–GFP co-immunoprecipitated

with Las17p–HA (Figure 2C), while Kre6pΔ1–GFP and Kre6pΔ2–GFP did not (data not shown).

Localization of Kre6p to cis-Golgi vesicles requires the cytoplasmic tail and is Las17p, Sla1p and Vrp1p-dependent

N-terminal fusions of GFP with the truncated constructs, Kre6pΔ1 and Kre6pΔ2 (Figure 1B and

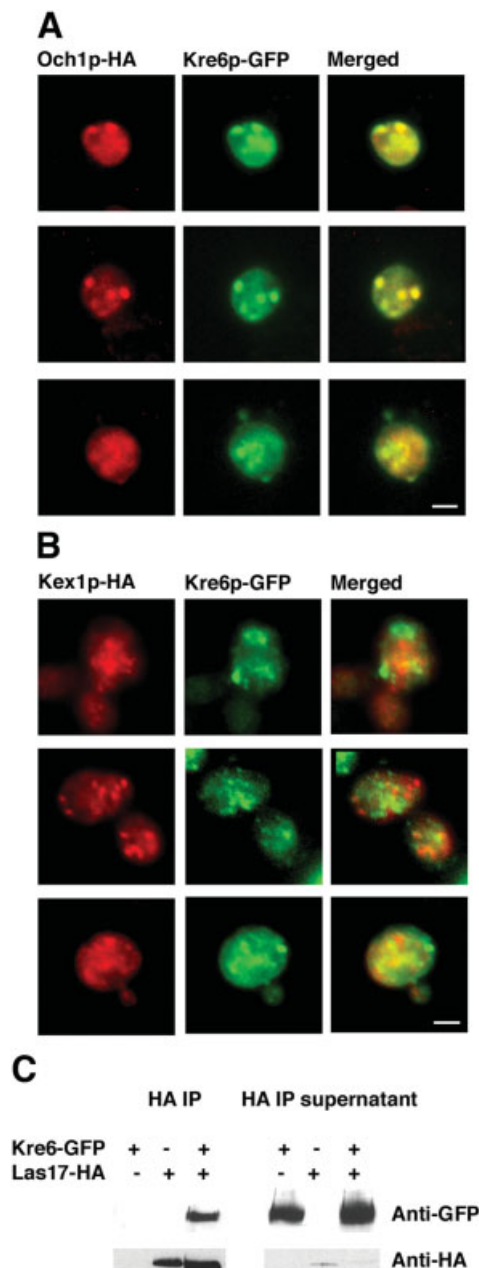


Figure 2. Kre6p shows extensive co-localization with the *cis*-Golgi protein, Och1p (A), but limited co-localization with the late Golgi protein Kex1p (B). Double immunofluorescence labelling of the Golgi proteins Kre6p and Och1p or Kex1p was performed as described in Materials and methods. Bars, 2 μ m. (C) Co-immunoprecipitation of Kre6p with Las17p. Extracts prepared from cells expressing Kre6p-GFP and Las17p-HA or from untagged controls were immunoprecipitated with anti-HA, as described in Materials and methods. Immunoprecipitated proteins and supernatants were detected by Western analysis against GFP (top) or HA (bottom)

Table 4. Two-hybrid interactions between the Kre6p cytoplasmic tail and Las17p and Sla1p

DNA-binding domain fusion	Activation domain fusion isolated from the screen	β -Galactosidase activity (units)
Kre6p (1–137 aa)	Las17p (168–400 aa)	118 \pm 12
	Las17p (168–400 aa)	278 \pm 22
	Sla1p (453–887 aa)	388 \pm 31
	Sla1p (475–576 aa)	336 \pm 29
	Sla1p (475–891 aa)	454 \pm 35

1–1.5 \times 10⁶ colonies were screened for protein interactions with the N-terminal 137 amino acid residues of the cytoplasmic tail of Kre6p, 65 positives were identified, and Las17p and Sla1p shown to be interacting proteins. β -Galactosidase assays were as described (Gietz *et al.*, 1997). Each value represents the average of two independent assays \pm SD. pGAD C1 was used as a vector control, and had a β -galactosidase activity of 0.4 \pm 0.1. The Skn1p cytoplasmic tail with the above fragments of Las17p and Sla1p had β -galactosidase activities at the same level as the vector control.

Table 2), were made to assess the requirement of the cytoplasmic tail for localization of Kre6p. Similar to their Kre6p counterparts, wild-type Kre6p-GFP, expressed from a centromeric plasmid, complemented the *kre6* null K1 toxin resistance phenotype, while Kre6p Δ 1-GFP partially complemented and Kre6p Δ 2-GFP did not. High copy plasmids were used for successful visualization. Overexpression of Kre6p-GFP in wild-type (212 cells examined) or *kre6* null mutant (153 cells examined) cells showed normal actin polarization in more than 90% of the cells (data not shown).

Wild-type Kre6p-GFP expressed from a 2 μ plasmid in *kre6* null and wild-type cells localized to the *cis*-Golgi in both mother and daughter cells (Figures 3A, 4A, B). When expressed in a *kre6* null, Kre6p Δ 1-GFP showed distinct *cis*-Golgi structures in less than 50% of the cells (Figure 3B). A fluorescence signal was absent from more than 90% of the cells expressing Kre6p Δ 2-GFP, with the remaining 10% of the cells showing a diffuse signal (Figure 3C); 250–300 cells were examined in each case. Similar results were observed when Kre6p Δ 1-GFP and Kre6p Δ 2-GFP were expressed in wild-type cells (data not shown), indicating that Kre6p Δ 1-GFP is still partially able to target the protein to its proper localization, while Kre6p Δ 2-GFP is not. Western analysis with anti-GFP antibody showed that there was much less protein

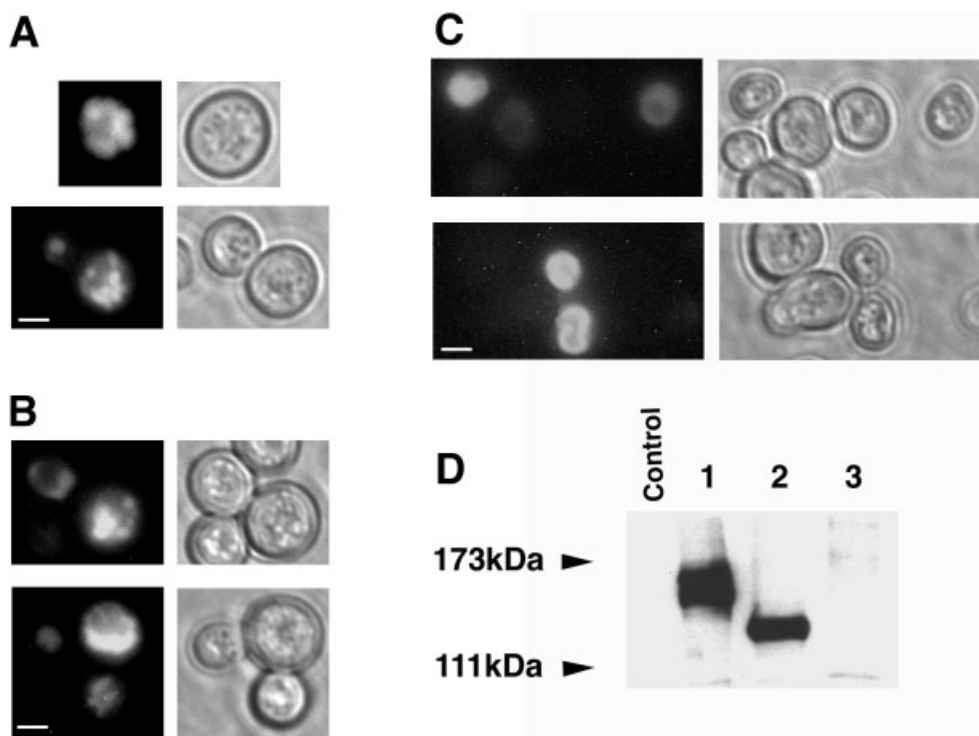


Figure 3. (A–C) Requirement of the Kre6p cytoplasmic tail for correct localization. Localization of Kre6p–GFP (A), Kre6p Δ 1–GFP (B) and Kre6p Δ 2–GFP (C) in a *kre6* Δ . (D) Detection of Kre6p–GFP (1), Kre6p Δ 1–GFP (2) and Kre6p Δ 2–GFP (3) in a *kre6* Δ . Control, Kre6p expressed in a *kre6* Δ . Protein loaded was standardized to the equivalent of 20 μ g total cellular protein. Bars, 2 μ m

detected in the cell lysates from the cells expressing Kre6p Δ 2–GFP in a *kre6* null, while both Kre6p–GFP and Kre6p Δ 1–GFP were more abundant when expressed in the same background (Figure 3D), suggesting that the second part of the cytoplasmic tail of the protein is possibly required for the stability of the protein.

The cytoplasmic tail is required for the proper localization of Kre6p–GFP and mediates the two-hybrid interaction with Las17p and Sla1p, so we tested whether these proteins were critical for Kre6p localization. Localization of Kre6p–GFP expressed from a 2μ -based plasmid was examined in *las17* Δ (Figure 4C) and *sla1* Δ cells (data not shown). Fluorescence microscopy revealed that Kre6p–GFP was mislocalized in 90% of *las17* Δ cells and 40% of *sla1* Δ cells (150 cells scored for each mutant). *cis*-Golgi structures containing Kre6p were absent from these cells, where a diffuse Kre6p signal was seen (Figure 4C). Las17p is known to physically interact with both Sla1p (Li, 1997) and Vrp1p (Naqvi *et al.*, 1998), and Kre6p–GFP

(2μ) localization was tested in a *vrp1* Δ deletion strain, with no *cis*-Golgi structures found in 80% of the cells (150 cells scored; data not shown). The *kre6* $\Delta*vrp1* Δ double mutant was found to be synthetically lethal (data not shown). Kre6p–GFP (2μ) was expressed at similar levels in wild-type, *kre6* Δ , *sla1* Δ , *vrp1* Δ and *las17* Δ strains (Figure 4D).$

To test whether these cortical actin assembly mutants disrupt *cis*-Golgi protein localization more widely, we examined localization of Och1p–HA (Harris and Waters, 1996) in wild-type, *las17* Δ , *sla1* Δ and *vrp1* Δ mutant cells. To test for more general membrane protein mislocalization in these mutants, we examined two plasma-membrane proteins, Mid2p–GFP and Fks1p–GFP, and three Golgi membrane proteins, the *medial*-Golgi protein Kre2p, the late-Golgi proteins Kex1p–HA and Chs5p–GFP (Lussier *et al.*, 1995; Santos and Snyder, 1997; Ketela *et al.*, 1999; Dijkgraaf *et al.*, 2002). Localization of each of these proteins in mutant cells resembled that of the wild-type, except

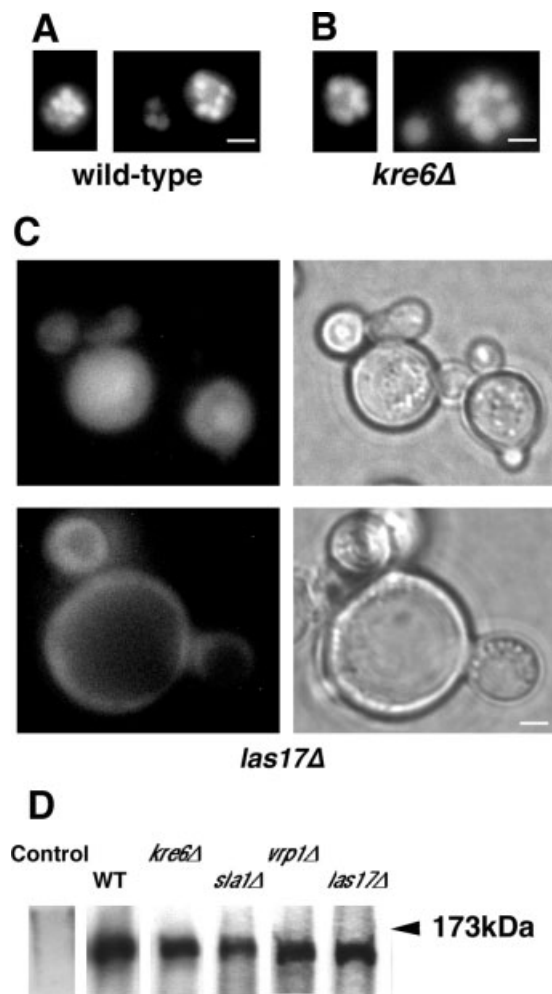


Figure 4. (A–C), Localization of Kre6p–GFP in wild-type (A), *kre6*Δ (B) and *las17*Δ (C). Phase contrast of the same *las17*Δ cells is shown in the right panel. (D) Detection of Kre6p–GFP in wild-type (WT), *kre6*Δ, *sla1*Δ, *vrp1*Δ and *las17*Δ mutants. Control, Kre6p expressed in a *kre6*Δ. Protein loaded was standardized to the equivalent of 24 μg total cellular protein. Bars, 2 μm

for Kex1p–HA, which was mislocalized (data not shown). Thus, while cortical actin assembly mutants do not appear to cause widespread membrane protein mislocalization, some, but not all, Golgi proteins are dependent on an intact actin cytoskeleton for their proper localization.

Actin patch assembly mutants have wall phenotypes

In an effort to functionally relate cell wall synthesis with actin patch assembly components,

Table 5. Cell wall glucan levels

Genotype	Alkali-insoluble glucan (%)	
	β-1,6-Glucan ^a	β-1,3-Glucan ^a
Wild-type	100 ± 4.9	100 ± 2.0
<i>kre6</i> Δ	35 ± 1.9	120 ± 7.4
<i>sla1</i> Δ	217 ± 18.1	77 ± 12.9
<i>las17</i> Δ	214 ± 3.3	136 ± 9.5
<i>she4</i> Δ	125 ± 4.0	86 ± 4.0

The levels of cell wall alkali-insoluble glucan were determined as described (Shahinian *et al.*, 1998). Values were calculated as μg of alkali-insoluble glucan/mg of total cellular protein, and are reported as percentages (wild-type = 100% with values of 90.8 ± 4.6 μg β-1,6-glucan, and 190.1 ± 4.1 μg β-1,3-glucan/mg cellular protein).

^a Values represent mean ± SD.

we screened a variety of cytoskeletal mutants for altered K1 killer toxin sensitivity. The actin patch assembly mutants, *arc18* Δ, *las17*Δ, *vrp1*Δ, *end3*Δ, *sac6*Δ, *sla1*Δ and *sla2*Δ, showed reduced toxin sensitivity, indicative of a possible cell wall defect, while other mutants in cytoskeletal components, such as *arp6*Δ, *bni1*Δ, *dec1*Δ, *myo3*Δ, *myo4*Δ, *rvs161*Δ, *rvs167*Δ and *twf1*Δ, had no phenotype. One cause of reduced toxin sensitivity comes from reduced β-1,6-glucan levels, as is found in a *kre6* null mutant (see Table 5). Cell wall glucan levels were determined in *las17*Δ and *sla1*Δ mutants and, unexpectedly, both showed twice the wild-type levels of β-1,6-glucan (Table 5, and see end of next section). A more modest elevation of β-1,6-glucan was also detected in *she4*Δ (Table 5), involved in actin polarization and mother–daughter polarity. To test whether the Kre6p mutants, Kre6pΔ1–GFP or Kre6pΔ2–GFP, unable to interact with Sla1p or Las17p, also showed overproduction of β-1,6-glucan, we determined the level of their glucan when these constructs were expressed in a *kre6*Δ mutant. The β-1,6-glucan levels were similar or below the level found in the wild-type (Figure 1B). In an additional test, overproduction of Kre6p in a *las17*Δ mutant had no effect on the β-1,6-glucan overproduction.

Actin patch assembly mutants show abnormal cell wall proliferation

Electron microscopy of actin patch assembly mutants with elevated cell wall glucan levels showed some cells with thick cell walls, a phenotype previously noted (Goodson *et al.*, 1996;

Mulholland *et al.*, 1997; Ayscough *et al.*, 1999; Tang *et al.*, 2000; Naqvi *et al.*, 2001), and in the case of cells overexpressing the Sla1p repeats, 48% of mother cells were affected (Tang *et al.*, 2000). To further assess the frequency and severity of this wall defect, we undertook a single-cell lineage analysis. Virgin daughter cells with null mutations in *LAS17*, *SLA1* or *VRP1* were capable of only a limited number of cell divisions compared to the wild-type (Figure 5). Wild-type cells underwent cell divisions by budding for over 20 cycles, while mutant cells became large and spherical and stopped budding on average after 5, 6 or 7 cycles for *las17* Δ , *sla1* Δ and *vrp1* Δ , respectively. Wild-type cells took slightly longer to divide after 15 cycles, while *las17* Δ , *sla1* Δ and *vrp1* Δ cells greatly slowed their divisions after three to four cycles, taking up to 6–8 h to complete a cell cycle. We attribute the K1 toxin resistance seen in these mutants to their thickened cell wall, which may act to block toxin access to the plasma membrane despite an increase in the amount of the β -1,6-glucan toxin receptor. Binding of toxin to the extra β -1,6-glucan in the thick walls may also act as a sink for the toxin, decreasing its effective concentration, and thus reducing toxin sensitivity.

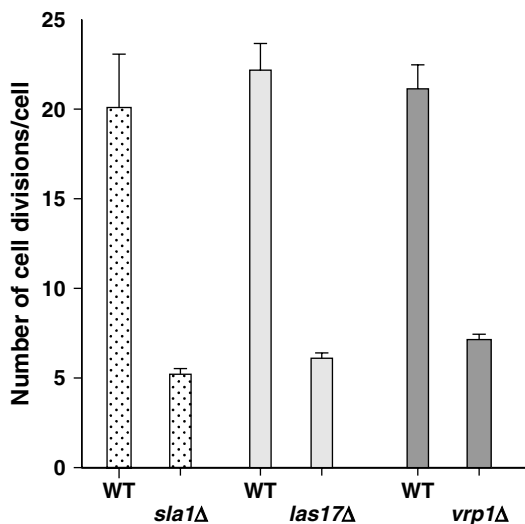


Figure 5. Single cell lineage analysis. In each strain, nine newly budded daughter cells were removed from their mothers and separated on YEPD agar. The total number of cell divisions of these virgin daughters were monitored by the removal and counting of each newly formed bud until no further budding occurred (see Materials and Methods)

Wall hypertrophy occurs by the addition of wall material in mother cells

The reduced number of cell divisions in these mutants simplified their population structures, allowing a quantitative analysis of the frequency of wall proliferation in cells. EM images showed that about 50% of the *las17* Δ , *sla1* Δ and *vrp1* Δ mother cells have thick walls. Analysis of hypertrophied mother cells revealed some with two-, three- or more-layered walls (Figure 6), with the proportion of these cells in the population equivalent to the presumed number of divisions they had undergone. Explicitly, 50% of the mother cells are normal with a one-layered wall, while 27% of cells have two layers, 13% have three layers and 10% have multi-layered walls. Buds newly generated from a mother cell with a three- or more-layered wall often contained a two-layered wall (Figure 7). These results are consistent with new wall deposition occurring in the mother cell at each round of budding. In wild-type cells, wall synthesis is restricted to the bud, with the mother cell having only a single cell wall, irrespective of the number of rounds of budding it has undergone (Figure 7).

Extra wall proliferation in mother cells results from new polymer synthesis

New wall synthesis is largely limited to the bud in growing yeast cells (Barral *et al.*, 2000). We asked if this mother–bud asymmetry was lost in *las17*, *sla1* and *vrp1* null mutants, leading to new cell wall synthesis in both mother and bud. To see where new β -1,6-glucan synthesis occurs in the cell, we adapted the procedure developed by Tkacz and Lampen (1972) to demonstrate new mannan synthesis. In this adapted procedure, pre-existing polymer was masked with an anti β -1,6-glucan antibody and a non-fluorescent secondary antibody. Following such masking, cells were allowed to grow and newly synthesized polymer localized using an anti β -1,6-glucan antibody and a fluorescent secondary antibody. Although not previously demonstrated, we found, as expected, that wild-type cells limit new synthesis of β -1,6-glucan to the daughter cell, with most of the fluorescence seen in buds, and with little or no signal seen in mother cells (Figure 8A–D). In contrast, in cells of *las17* (Figure 8E–H), *sla1* and *vrp1* null mutants (data not shown) new β -1,6-glucan was deposited in both buds and mother cells. These

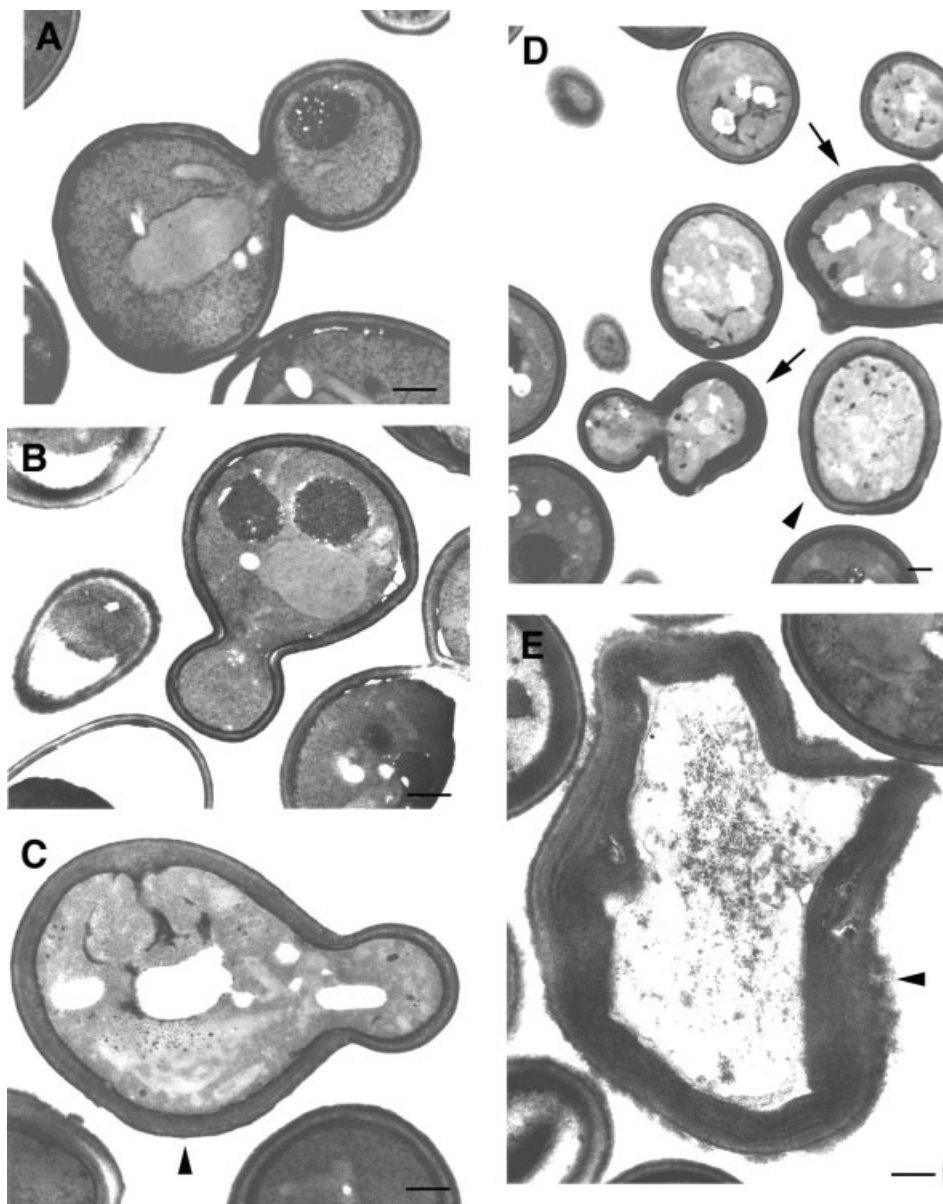


Figure 6. Electron micrographs showing cell wall ultrastructure in cells grown in YEPD liquid medium at room temperature. (A) wild-type, showing a single-layered wall in both mother and daughter cells. (B) *las17* Δ , showing a single-layered wall in both mother and daughter cells. (C) *vrp1* Δ , showing a two-layered wall in the mother (arrowhead) and a single-layered wall in the daughter cell. (D) *vrp1* Δ , showing a range of cells of varying cell wall thickness (arrowhead, two-layered wall, arrows, three-layered walls). (E) *las17* Δ , showing a multi-layered wall (arrowhead). Bars, 500 nm

results indicate that the new wall polymer deposition is no longer restricted to the bud, and that the mother cell wall hypertrophy seen in mutants results from a loss of asymmetric synthesis of new cell wall material. To address a possible role of Kre6p in establishing asymmetry in cell wall synthesis, we determined the sites of new β -1,6-glucan

deposition in *kre6* Δ and in the cytoplasmic tail deletions Kre6p Δ 1-GFP and Kre6p Δ 2-GFP. In all cases we found that new glucan synthesis was restricted to daughter cells (data not shown). Thus, the loss of asymmetric β -1,6-glucan synthesis seen in *las17* Δ and *sla1* Δ mutants involves more than the interaction of Las17p and Sla1p with Kre6p.




Type of cells	Wall layers in mother	Percentage in the population				
		<i>las17Δ</i> n=309	<i>sla1Δ</i> n=266	<i>vrp1Δ</i> n=277	Average	WT n=300
	one	50	51	48	50 ± 2	100
	two	26	29	27	27 ± 2	0
	three	12	12	14	13 ± 1	0
	more	12	8	11	10 ± 2	0

Figure 7. Wall proliferation distributions in wild-type, *las17Δ*, *sla1Δ* and *vrp1Δ* mutant populations. Cells were grouped according to the number of cell wall layers in mother cells, as seen under EM. n, total number of cells counted

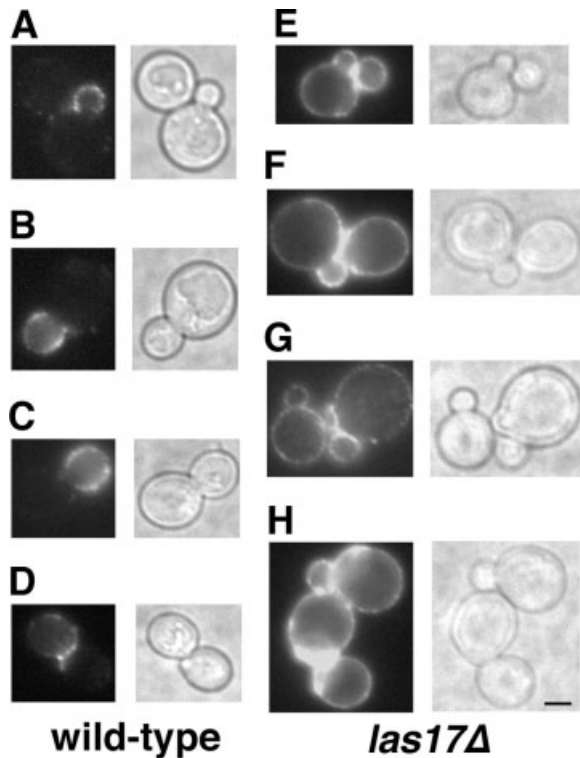


Figure 8. Localization of newly synthesized β -1,6-glucan in wild-type and *las17Δ* cells. (A–D) New deposition of β -1,6-glucan in wild-type daughter cells (left panels). (E–F) New deposition of β -1,6-glucan in mother and daughter cells in *las17Δ* (left panels). Phase contrast images of the same cells are also shown (right panels). Bar, 2 μ m

Discussion

S. cerevisiae Kre6p is a *cis*-Golgi membrane protein with a luminal glucosyl hydrolase-like domain

and an N-terminal cytoplasmic domain that interacts with Las17p and Sla1p. Thus, Kre6p appears to be bi-functional, with its cytoplasmic domain acting as a receptor and the luminal glycoside hydrolase domain functioning in β -glucan biogenesis. The cytoplasmic tail of Kre6p is required for its activity and localization, and interacts in a two-hybrid assay with Las17p and Sla1p, two proteins that themselves interact directly in a protein complex. The Kre6p interactions seem biologically relevant, as Kre6p–GFP is mislocalized in both *las17Δ* and *sla1Δ* mutants in a manner similar to the Kre6p Δ 1–GFP and Kre6p Δ 2–GFP fusion protein mutants, in which the tail of Kre6p has been partially or completely deleted. Mislocalization of Kre6p in these actin patch assembly mutants shows some specificity, since most other Golgi membrane and plasma membrane proteins examined have normal localization. The co-immunoprecipitation of Kre6p–GFP with Las17p–HA, the requirement of the cytoplasmic tail for such associations, and the finding that the *kre6Δlas17Δ* and *kre6Δsla1Δ* double mutants are synthetically lethal, implicate the cytoplasmic tail of Kre6p as a receptor coupling this *cis*-Golgi protein to the actin assembly machinery.

The direct binding of a vesicle protein to the actin assembly complex is an unexpectedly simple solution to the receptor-targeting problem. A related example of direct coupling has recently been found, where the cytoplasmic domain of the *Drosophila* post-Golgi vesicle protein, Sunday Driver, a homologue of the proposed mammalian JNK scaffolding protein, JIP-3, interacts with the kinesin light chain of kinesin-I and is required for

normal axonal vesicle trafficking (Bowman *et al.*, 2000; Verhey *et al.*, 2001). Such targeting via the direct interaction of vesicles through the cytoplasmic tails of their resident membrane proteins with cytoskeletal elements is intriguing, and may be common but overlooked because of technical difficulties in showing protein–protein interactions with membrane proteins.

Our results address and relate two themes: the targeting of secretory vesicles and the loss of regulation of wall deposition in mutants with defects in actin assembly. Mutant cells with multi-layered walls have often been seen (Goodson *et al.*, 1996; Mulholland *et al.*, 1997; Marcoux *et al.*, 1998; Stolz *et al.*, 1998; Ayscough *et al.*, 1999; Tang *et al.*, 2000; Naqvi *et al.*, 2001), although their cause is uncertain. Cell lineage experiments and EM image analysis allowed a detailed study of this hypertrophy. Single cell lineages showed that mutant cells of *las17* Δ , *sla1* Δ and *vrp1* Δ can undergo only a limited number of cell divisions. However, bud initiation and septum formation appear normal, suggesting that these polarized events in cell wall synthesis are unaffected. Quantitative analysis of EM images showed that approximately 50% of the *las17* Δ , *sla1* Δ and *vrp1* Δ cells have abnormal wall proliferation in mother cells. The result is consistent with a mother cell acquiring additional wall material with every division when the daughter is undergoing cell wall growth, commencing with the onset of wall growth in the first daughter cell. The deposition pattern of new cell wall material in the mother cell is not polarized and is consistent with isotropic growth, although we have not addressed the nature of wall deposition in the growing bud in these mutants. Studies on the sites of new wall synthesis have shown that both mannoprotein and chitin are laid down predominantly, if not exclusively, in buds or newly separated daughter cells (Tkacz and Lampen, 1972; Santos and Snyder, 1997). Our work to visualize the sites of deposition of newly synthesized β -1,6-glucan in wild-type cells concurs with these previous studies; however, in *las17* Δ , *sla1* Δ and *vrp1* Δ cells, new localization of β -1,6-glucan is not restricted to the bud but also occurs in mother cells.

As a consequence of their actin assembly defects, *las17* Δ , *sla1* Δ and *vrp1* Δ mutants cannot undergo endocytosis, and it has been proposed that this lack of endocytosis could cause wall proliferation (Mulholland *et al.*, 1997; Pruyne and Bretscher, 2000).

Perhaps there is normally a large-scale removal of the biosynthetic machinery or remodelling of the mother wall through endocytosis, and that failure to achieve this turnover of biosynthetic or wall material leads to mother wall hypertrophy. This model suggests that the cell wall biosynthetic machinery would be localized to the plasma membrane of both mother and daughter cells, thus endocytosis is required to remove newly synthesized material or cell wall synthesis components from the mother cells. One prediction from an endocytosis model is that any defect in endocytosis should lead to a wall hypertrophy phenotype. We have examined other endocytosis mutants, using K1 toxin sensitivity as a primary phenotype. While an *end3* null mutant is partially resistant and does show the defect, other mutants show normal toxin sensitivity, and two of these, *rvs161* Δ and *rvs167* Δ , have been directly shown not to have wall proliferation defects (Tang *et al.*, 2000; Breton *et al.*, 2001). Thus, lack of endocytosis *per se* seems not to be sufficient for aberrant wall proliferation to occur. Experiments to examine deposition of new cell wall material show that new synthesis is restricted to the wild-type daughter cell. Our experiments do not eliminate the idea of removal of biosynthetic machinery such as Kre6p by a subset of endocytotic components such as Las17p and Sla1p. However, we prefer a model in which wall hypertrophy in actin patch assembly mutants results from a failure to directly restrict cortical actin assembly and the associated wall synthetic machinery to the bud. Whatever the mechanism, mother cells in such mutants then follow a catastrophic path, adding new wall material each generation and forming multi-layered walls that become incapable of further budding after 5–7 cycles (Figures 5, 7).

What are the components restricting wall growth to daughter cells? Abnormal mother wall proliferation is not a general defect of the cytoskeleton or cytoskeletal assembly components, but limited to a subset of actin patch assembly components. Wall proliferation is also an allele-specific phenotype of some actin mutants (Tang *et al.*, 2000), arguing that failure to limit cortical actin to the daughter is at the root of the problem. Another pertinent mutant with this phenotype is *she4* Δ . She4p is involved in actin polarization (Wendland *et al.*, 1996) and required for preferential accumulation of *ASH1* mRNA in daughter cells (Long *et al.*, 1997). Proper localization of *ASH1* mRNA depends partially on the

integrity of the actin cytoskeleton (Long *et al.*, 1997; Takizawa *et al.*, 1997). Wall defects of the *she* Δ mutant suggest that She4p is also required for limiting localization of cell wall synthesis to daughter cells.

Expression of Kre6p mutants, Kre6p Δ 1–GFP or Kre6p Δ 2–GFP in a *kre6* null did not show overproduction of β -1,6-glucan, and new glucan synthesis was restricted to daughter cells in these strains. The loss of asymmetric β -1,6-glucan synthesis seen in *las17* Δ and *sla1* Δ mutants thus involves more than the interaction of Las17p and Sla1p with Kre6p.

In conclusion, the cytoplasmic tail of Kre6p acts as a receptor, coupling this *cis*-Golgi protein with Las17p and Sla1p, proteins involved in actin organization and asymmetry establishment along the mother–daughter cell axis.

Acknowledgements

We thank Peter Dijkgraaf, Charlie Boone, Terry Roemer, Josh Levinson and Federico Angioni for discussions and constructs, Neta Dean, Troy Ketela, Marc Lussier and M. Gerard Waters for constructs, Jeannie Mui for electron microscopy and Patrice Ménard, Anne-Marie Sdicu and Maude Beaulieu for sequencing and killer assays. Supported by an NSERC Operating Grant to HB; HL was a FRSQ postdoctoral fellow.

References

- Anderson BL, Boldogh I, Evangelista M, Boone C, Greene LA, Pon LA. 1998. The Src homology domain 3 (SH3) of a yeast type I myosin, Myo5p, binds to verprolin and is required for targeting to sites of actin polarization. *J Cell Biol* **141**: 1357–1370.
- Ayscough KR, Eby JJ, Lila T, Dewar H, Kozminski KG, Drubin DG. 1999. Sla1p is a functionally modular component of the yeast cortical actin cytoskeleton required for correct localization of both Rho1p-GTPase and Sla2p, a protein with talin homology. *Mol Biol Cell* **10**: 1061–1075.
- Barral Y, Mermall V, Mooseker MS, Snyder M. 2000. Compartmentalization of the cell cortex by septins is required for maintenance of cell polarity in yeast. *Mol Cell* **5**: 841–851.
- Bowman AB, Kamal A, Ritchings BW, *et al.* 2000. Kinesin-dependent axonal transport is mediated by the Sunday driver (SYD) protein. *Cell* **103**: 583–594.
- Bradford MM. 1976. A rapid and sensitive method for the quantitation of microgram quantities of protein utilizing the principle of protein–dye binding. *Anal Biochem* **72**: 248–254.
- Breton AM, Schaeffer J, Aigle M. 2001. The yeast Rvs161 and Rvs167 proteins are involved in secretory vesicles targeting the plasma membrane and in cell integrity. *Yeast* **18**: 1053–1068.
- Brown JL, Kossaczka Z, Jiang B, Bussey H. 1993. A mutational analysis of killer toxin resistance in *Saccharomyces cerevisiae* identifies new genes involved in cell wall (1 \rightarrow 6)- β -glucan synthesis. *Genetics* **133**: 837–849.
- Bussey H, Sacks W, Galley D, Saville D. 1982. Yeast killer plasmid mutations affecting toxin secretion and activity and toxin immunity function. *Mol Cell Biol* **2**: 346–354.
- Chen DC, Yang BC, Kuo TT. 1992. One step transformation of yeast in stationary phase. *Curr Genet* **21**: 83–84.
- Chien C, Bartel PL, Fields S. 1991. The two-hybrid system: a method to identify and clone genes for proteins that interact with a protein of interest. *Proc Natl Acad Sci USA* **88**: 9578–9582.
- Christianson TW, Sikorski RS, Dante M, Shero JH, Hieter P. 1992. Multifunctional yeast high-copy-number shuttle vectors. *Gene* **110**: 119–122.
- Dijkgraaf GJP, Abe M, Ohya Y, Bussey H. 2002. Mutations in Fks1p affect the cell wall content of β -1,3- and β -1,6-glucan in *Saccharomyces cerevisiae*. *Yeast* **19**: 671–690.
- Evangelista M, Klebl BM, Tong AHY, *et al.* 2000. A role for myosin-I in actin assembly through interactions with Vrp1p, Bee1p, and the Arp2/3 complex. *J Cell Biol* **148**: 353–362.
- Fromont-Racine M, Rain J-C, Legrain P. 1997. Towards a functional analysis of the yeast genome through exhaustive two-hybrid screens. *Nature Genet* **16**: 277–282.
- Gietz RD, Schiestl RH, Willems AR, Woods RA. 1995. Studies of the transformation of intact yeast cells by the LiAc/SS-DNA/PEG procedure. *Yeast* **11**: 355–360.
- Gietz RD, Triggs-Raine B, Robbins A, Graham KC, Woods RA. 1997. Identification of proteins that interact with a protein of interest: applications of the yeast two-hybrid system. *Mol Cell Biochem* **172**: 67–79.
- Goodson H, Anderson B, Warrick H, Pon L, Spudich J. 1996. Synthetic lethality screen identifies a novel yeast myosin I gene (*MYO5*): myosin I proteins are required for polarization of the actin cytoskeleton. *J Cell Biol* **133**: 1277–1291.
- Gyuris J, Golemis E, Chertkov H, Brent R. 1993. Cdi1, a human G₁ and S phase protein phosphatase that associates with Cdk2. *Cell* **75**: 791–803.
- Harris SL, Waters MG. 1996. Localization of a yeast early Golgi mannosyltransferase, Och1p, involves retrograde transport. *J Cell Biol* **132**: 985–998.
- Hoffman CS, Winston F. 1987. A ten minute DNA preparation from yeast efficiently releases autonomous plasmids for transformation of *E. coli*. *Gene* **57**: 267–272.
- Igual JC, Johnson AL, Johnson LH. 1996. Coordinated regulation of gene expression by the cell cycle transcription factor Swi4 and the protein kinase C MAP kinase pathway for yeast cell integrity. *EMBO J* **15**: 5001–5013.
- Jungmann J, Munro S. 1998. Multi-protein complexes in the *cis*-Golgi of *Saccharomyces cerevisiae* with α -1,6-mannosyltransferase activity. *EMBO J* **17**: 423–434.
- Ketela T, Green R, Bussey H. 1999. *Saccharomyces cerevisiae* Mid2p is a potential cell wall stress sensor and upstream activator of the *PKC1*–*MPK1* cell integrity pathway. *J Bacteriol* **181**: 3330–3340.
- Kollár R, Reinhold BB, Petráková E, *et al.* 1997. Architecture of the yeast cell wall: β (1 \rightarrow 6)-glucan interconnects mannoprotein, β (1 \rightarrow 3)-glucan and chitin. *J Biol Chem* **272**: 17762–17775.

- Kunkel TA, Roberts JD, Zakour RA. 1987. Rapid and efficient site-specific mutagenesis without phenotypic selection. *Methods Enzymol* **154**: 367–382.
- Laemmli UK. 1970. Cleavage of structural proteins during the assembly of the head of bacteriophage T4. *Nature* **227**: 680–685.
- Li R. 1997. Bee1, a yeast protein with homology to Wiscott–Aldrich syndrome protein, is critical for the assembly of cortical actin cytoskeleton. *J Cell Biol* **136**: 649–658.
- Long RM, Singer RH, Meng X, Gonzalex I, Nasmyth K, Jansen RP. 1997. Mating type switching in yeast controlled by asymmetric localization of *ASH1* mRNA. *Science* **277**: 383–387.
- Lussier M, Sdicu A-M, Ketela T, Bussey H. 1995. Localization and targeting of the *Saccharomyces cerevisiae* Kre2p/Mnt1p α 1,2-mannosyltransferase to a medial-Golgi compartment. *J Cell Biol* **131**: 913–927.
- Lussier M, Sdicu A-M, Shahinian S, Bussey H. 1998. The *Candida albicans* *KRE9* gene is required for cell wall synthesis and is essential for growth on glucose. *Proc Natl Acad Sci USA* **95**: 9825–9830.
- Marcoux N, Bourbonnais Y, Charest PM, Pallotta D. 1998. Overexpression of *MID2* suppresses the profilin deficient phenotype of yeast cells. *Mol Microbiol* **29**: 515–526.
- Montijn RC, Vink E, Muller WH, et al. 1999. Localization of synthesis of β -1,6-glucan in *Saccharomyces cerevisiae*. *J Bacteriol* **181**: 7414–7420.
- Mulholland J, Wesp A, Riezman H, Botstein D. 1997. Yeast actin cytoskeleton mutants accumulate a new class of Golgi-derived secretory vesicle. *Mol Biol Cell* **8**: 1481–1499.
- Naqvi SN, Zahn R, Mitchell DA, Stevenson BJ, Munn AL. 1998. The WASP homologue Las17p functions with the WIP homologue End5p/verprolin and is essential for endocytosis in yeast. *Curr Biol* **8**: 959–962.
- Naqvi SN, Feng Q, Boulton VJ, Zahn R, Munn AL. 2001. Vrp1p functions in both actomyosin ring-dependent and Hof1p-dependent pathways of cytokinesis. *Traffic* **2**: 189–201.
- Poster JB, Dean N. 1996. The yeast *VRG4* gene is required for normal Golgi functions and defines a new family of related genes. *J Biol Chem* **271**: 3837–3845.
- Pruyne D, Bretscher A. 2000. Polarization of cell growth in yeast. II. The role of the cortical actin cytoskeleton. *J Cell Sci* **113**: 571–585.
- Roemer T, Bussey H. 1991. Yeast β -glucan synthesis: *KRE6* encodes a predicted type II membrane protein required for glucan synthesis *in vivo* and for glucan synthase activity *in vitro*. *Proc Natl Acad Sci USA* **88**: 11 295–11 299.
- Roemer T, Delaney S, Bussey H. 1993. *SKN1* and *KRE6* define a pair of functional homologs encoding putative membrane proteins involved in β -glucan synthesis. *Mol Cell Biol* **13**: 4039–4048.
- Roemer T, Paravicini G, Payton MA, Bussey H. 1994. Characterization of the yeast (1 \rightarrow 6)- β -glucan biosynthetic components, Kre6p and Sknlp, and genetic interactions between the PKC1 pathway and extracellular matrix assembly. *J Cell Biol* **127**: 567–579.
- Sambrook J, Fritsch EF, Maniatis T. 1989. *Molecular Cloning: a Laboratory Manual*, 2nd edn. Cold Spring Harbor Laboratory Press: New York.
- Santos B, Snyder M. 1997. Targeting of chitin synthase 3 to polarized growth sites in yeast requires Chs5p and Myo2p. *J Cell Biol* **136**: 95–110.
- Shahinian S, Dijkgraaf GJP, Sdicu A-M, et al. 1998. Involvement of protein *N*-glycosyl chain glucosylation and processing in the biosynthesis of cell wall β -1,6-glucan of *Saccharomyces cerevisiae*. *Genetics* **149**: 843–856.
- Sherman F, Fink D, Hicks JB. 1982. *Methods in Yeast Genetics*. Cold Spring Harbor Laboratory Press: New York.
- Sikorski RS, Hieter P. 1989. A system of shuttle vectors and yeast host strains designed for efficient manipulation of DNA in *Saccharomyces cerevisiae*. *Genetics* **122**: 19–27.
- Spellman PT, Sherlock G, Zhang MQ, et al. 1998. Comprehensive identification of cell cycle-regulated genes of the yeast *Saccharomyces cerevisiae* by microarray hybridization. *Mol Biol Cell* **9**: 3273–3297.
- Srinivasan S, Seaman M, Nemoto Y, et al. 1997. Disruption of three phosphatidylinositol-polyphosphate 5-phosphatase genes from *Saccharomyces cerevisiae* results in pleiotropic abnormalities of vacuole morphology, cell shape, and osmohomeostasis. *Eur J Cell Biol* **74**: 350–360.
- Stolz LE, Huynh CV, Thorner J, York JD. 1998. Identification and characterization of an essential family of inositol polyphosphate 5-phosphatases (*INP51*, *INP52* and *INP53* gene products) in the yeast *Saccharomyces cerevisiae*. *Genetics* **148**: 1715–1729.
- Takizawa PA, Sil A, Swedlow JR, Herskowitz I, Vale RD. 1997. Actin-dependent localization of an RNA encoding a cell-fate determinant in yeast. *Nature* **389**: 90–93.
- Tang H, Xu J, Cai M. 2000. Pan1p, End3p, and Sla1p, three yeast proteins required for normal cortical actin cytoskeleton organization, associate with each other and play essential roles in cell wall morphogenesis. *Mol Cell Biol* **20**: 12–25.
- Tkacz JS, Lampen JO. 1972. Wall replication in *Saccharomyces* species: use of fluorescein-conjugated concanavalin A to reveal the site of mannan insertion. *J Gen Microbiol* **72**: 243–247.
- Verhey KJ, Meyer D, Deehan R, et al. 2001. Cargo of kinesin identified as JIP scaffolding proteins and associated signaling molecules. *J Cell Biol* **152**: 959–970.
- Wach A, Brachat A, Pöhlmann R, Philippsen P. 1994. New heterologous modules for classical PCR-based gene disruption in *Saccharomyces cerevisiae*. *Yeast* **10**: 1793–1808.
- Wendland B, McCaffery JM, Xiao Q, Emr SD. 1996. A novel fluorescence-activated cell sorter-based screen for yeast endocytosis mutants identifies a yeast homologue of mammalian eps15. *J Cell Biol* **135**: 1485–1500.